Hindawi
Discrete Dynamics in Nature and Society
Volume 2024, Article ID 5580918, 19 pages
https://doi.org/10.1155/2024/5580918

Research Article

Numerical Analysis and Computation of a Subgrid-Sparse-Grad-Div Stabilization Method for Incompressible Flow Problems

Yun-Bo Yang [1,2,3] **and Bin-Chao Huang** [1]

[1] *Department of Mathematics, Yunnan Normal University, Kunming 650500, China*
[2] *Yunnan Key Laboratory of Modern Analytical Mathematics and Applications, Yunnan Normal University, Kunming 650500, China*
[3] *Key Laboratory of Complex System Modeling and Application for Universities in Yunnan, Yunnan Normal University, Kunming 650500, China*

Correspondence should be addressed to Bin-Chao Huang; bchuang18@126.com

Received 27 January 2023; Revised 15 February 2024; Accepted 21 February 2024; Published 13 March 2024

Academic Editor: Francisco R. Villatoro

In this article, a subgrid-sparse-grad-div method for incompressible flow problem was proposed, which is a combination of the subgrid stabilization method and the recently proposed sparse-grad-div method. The method maintains the advantage of both methods: (i) It is robust for solving incompressible flow problem with dominance of the convection, especially when the viscosity is too small. (ii) It can keep mass conservation. Therefore, the method is very efficient for solving incompressible flow. Moreover, based on the Crank–Nicolson extrapolated scheme for temporal discretization, and mixed finite element in spatial discretization, we derive the unconditional stability and optimal convergence of the method. Finally, numerical experiments are proposed to validate the theoretical predictions and demonstrate the efficiency of the method on a test problem for incompressible flow.

1. Introduction

In this paper, we consider the incompressible time-dependent Navier–Stokes (NS) equations. For a bounded, regular domain $\Omega \subset \mathbb{R}^d$ ($d = 2$ or 3), we find u: $\Omega \times [0, T] \longrightarrow \mathbb{R}^d$ and p: $\Omega \times [0, T] \longrightarrow \mathbb{R}$ satisfying

$$\begin{aligned} u_t + \nu\Delta u + (u \cdot \nabla)u + \nabla p &= f \text{ in } \Omega \times [0, T], \\ \nabla \cdot u &= 0 \text{ in } \Omega \times [0, T], \\ u &= 0 \text{ on } \partial\Omega \times [0, T], \\ u(0, \cdot) &= u_0(x) \; for \; x \in \Omega, \end{aligned} \tag{1}$$

where u and p represent the fluid velocity and zero-mean pressure, respectively, ν represents the kinematic viscosity, and f and u_0 are the prescribed terms.

System (1) provides a mathematical model of incompressible Newtonian viscous fluid flow. They can describe many important physical phenomena such as weather prediction or climate modeling, flow around airfoils, ocean current, and blood flow in the arteries. Therefore, it is of practical interest to design efficient numerical methods for solving NS equations. Among the numerical methods, the Galerkin finite element method is a popular method, for more details, see [1–3] and references therein. However, the

numerical solution solved by using finite methods often suffer from spurious oscillations and inaccurate approximation, the main reason for this is the fact that dominance of the convection, especially when the viscosity is too small, or the poor mass conservation. In order to deal with these effects, various stabilization techniques have been proposed.

Among these stabilization methods, one of the most popular stabilization methods applied on incompressible flow problems is the variational multiscale (VMS) method, which is based on the decomposition of the flow scales. In a type of VMS method, the flow is decomposed into the large scales and small scales, and the former is defined by projection into appropriate subspaces. For more details, we can see [4–8] and the references therein. The subgrid stabilization method is an improvement of the VMS method, which uses the two-grid techniques [9–11], and assumes that there exist fine scales and coarse scales of the flow. The main ideas of subgrid stabilization method are to first add an artificial viscosity term on a fine scales and then subtract it off only on the coarse scales, see, for example [12–14]. It has ample applications about subgrid stabilization method, such as steady-state natural convection problem [15], the incompressible magnetohydrodynamics (MHD) [16], and Darcy–Brinkman equations in double-diffusive convection [17], optimal control of the unsteady Navier–Stokes equations [18], and so on. The grad-div stabilization method is another popular stabilization method, which was studied in [19–21]. It can be look as the penalized stabilization of the divergence constraint. Since using the common finite element methods does not give divergence-free solutions, the divergence constraint condition is damaged severely [19]. When adding the grad-div term as a penalty term with respect to the continuity equation, it can improve the conservation of mass. The significant feature of the method is that it enhances the discrete mass conservation and reduces the effect of the pressure error on the velocity error.

Recently, a new grad-div type stabilization technique, namely, the sparse-grad-div stabilization method, was derived in [22]. The stabilization term added in this method produces block upper triangular matrices in two dimensions case and in three dimensions, the 2, 1 and 3, 1 blocks are empty. Since the sparser structure of its matrices, this new grad-div method not only can achieve the same positive effect compare with the common grad-div method but also is more efficient. The new grad-div method was extended to solve Navier–Stokes equations with a projection algorithm [23] and to solve optimal control problem of stationary Navier–Stokes equations [24]. The other variant of the grad-div stabilization can be seen in [25–27].

The main contribution of this work is to derive a synthesized stabilization finite element method for solving incompressible flow problem. This method is a combination of the subgrid stabilization method and the recently proposed sparse-grad-div method and possesses the advantage of both methods. It is robust for solving incompressible flow problems with dominance of the convection, especially when the viscosity is too small. In addition, it can keep mass conservation. Therefore, the method is very efficient for solving incompressible flow. Moreover, based on the Crank–Nicolson extrapolated scheme for temporal discretization, and mixed finite element in spatial discretization, we derive the unconditional stability and optimal convergence of the method. Numerical experiments are proposed to validate the theoretical predictions and demonstrate the efficiency of the method on a test problem for incompressible flow.

The article is arranged as follows. Section 2 introduces some notations and preliminary results that will be used throughout this article, and presents the numerical algorithm. In Section 3, we prove the unconditional stability of the proposed method. In Section 4, we perform a rigorous error analysis of the presented algorithm. A series of numerical experiments are provided to verify the efficiency of the method in Section 5. Finally, we conclude the article.

2. Mathematical Preliminaries

We first generalize some notations, definitions, and preliminary lemmas which will be used in the analysis. Let $\Omega \subset \mathbb{R}^d$ ($d = 2$ or 3) be an open, bounded convex polygonal or polyhedra domain, with a Lipschitz-continuous boundary $\partial\Omega$. The inner product on $L^2(\Omega)$ or $L^2(\Omega)^{d\times d}$, the norm in $L^2(\Omega)$, and the norm in $L^\infty(\Omega)$ are denoted by $(\cdot,\cdot)$, $\|\cdot\|$, and $\|\cdot\|_\infty$, respectively. Likewise, the $L^p(\Omega)$ norms and the Sobolev space $W_p^k(\Omega)$norms are denoted by $\|\cdot\|_{L^p}$ and $\|\cdot\|_{W_p^k}$, respectively. For the seminorm in $W_p^k(\Omega)$, we denote it by $|\cdot|_{W_p^k}$. $H^k(\Omega)$ is the standard Hilbertian Sobolev space of order k with norm $\|\cdot\|_k$. For the given function, $v(x,t)$ defined on the entire time interval $(0,T)$, we define the norm

$$\begin{aligned} \|v\|_{\infty,k} &= \sup_{0<t<T} \|v(\cdot,t)\|_k, \\ \|v\|_{m,k} &= \left(\int_0^T \|v(\cdot,t)\|_k^m dt\right)^{1/m}. \end{aligned} \tag{2}$$

For the mathematical setting of problem (1), the following Sobolev spaces for the velocity u, the pressure p are introduced, respectively, by

$$\begin{aligned} X &= H_0^1(\Omega)^d = \left\{v \in H^1(\Omega)^d\colon\ v = 0 \text{ on } \partial\Omega\right\}, \\ M &= L_0^2(\Omega) = \left\{\varphi \in L^2(\Omega)\colon \int_\Omega \varphi dx = 0\right\}, \end{aligned} \tag{3}$$

where the space X is equipped with the L^2-scalar product $(\cdot,\cdot)$ and the norm $\|\cdot\|$, and the space M is equipped with the usual L^2-norm. Finally, the space $H^{-1}(\Omega)$, the dual space of $H_0^1(\Omega)$, is equipped with the negative norm

$$\|f\|_{-1} = \sup_{v\in H_0^1(\Omega)} \frac{|(f,v)|}{\|\nabla v\|}. \tag{4}$$

In addition, the classical space of divergence-free functions is defined by

$$V = \{v \in X\colon\ (\varphi, \nabla\cdot v) = 0 \quad \forall \varphi \in M\}. \tag{5}$$

With above notations, we can get the weak formulation of (1) as follows: Find $u\colon [0,T] \longrightarrow X$, $p\colon [0,T] \longrightarrow M$ for a.e. $t \in (0,\ T]$ satisfying

$$\begin{aligned}(u_t, v) + \nu(\nabla u, \nabla v) + b^*(u,u,v) - (p, \nabla\cdot v) &= (f, v) \quad \forall v \in X,\\ (\nabla\cdot u, q) &= 0 \quad \forall q \in M,\end{aligned} \tag{6}$$

where the skew symmetrized trilinear form is defined as follows:

$$b^*(u,v,w) = \frac{1}{2}(u\cdot\nabla v, w) - \frac{1}{2}(u\cdot\nabla w, v) \quad \forall u,v,w \in X. \tag{7}$$

By the divergence theorem, we know

$$b^*(u,v,w) = \int_\Omega u\cdot\nabla v\cdot w\,\mathrm{d}x + \frac{1}{2}\int_\Omega (\nabla\cdot u)(v\cdot w) \quad \forall u,v,w \in X. \tag{8}$$

We also note that

$$b^*(u,v,v) = 0 \quad \forall u,v \in X. \tag{9}$$

The trilinear form has the following bounds, see [1, 3] for more details,

$$|b^*(u,v,w)| \le C\|\nabla u\|\|\nabla v\|\|\nabla w\| \quad \forall u,v,w \in X, \tag{10}$$

$$\begin{aligned}|b^*(u,v,w)| &\le C\|u\|^{1/2}\|\nabla u\|^{1/2}\|\nabla v\|\|\nabla w\| \quad \forall u,v,w \in X,\\ |b^*(u,v,w)| &\le C\|\nabla u\|\|\nabla v\|\|w\|^{1/2}\|\nabla w\|^{1/2} \quad \forall u,v,w \in X.\end{aligned} \tag{11}$$

In addition, if $v, \nabla v \in L^\infty(\Omega)$, we have (see e.g., Lemma 1 in [28]).

$$|b^*(u,v,w)| \le C\|u\|\left(\|v\|_\infty + \|\nabla v\|_\infty\right)\|\nabla w\| \quad \forall u,w \in X. \tag{12}$$

2.1. Finite Element Approximation. We now introduce the finite element discretization of (6). Let $\tau_h = \{\Omega_h\}$ and $\tau_H = \{\Omega_H\}$ are two uniformly regular triangulation of domain Ω into triangular in $\mathbb{R}^2$ or tetrahedral in $\mathbb{R}^3$. Thus, the computational domain is defined by

$$\Omega = \bigcup K \quad \forall K \in \tau_h(\text{resp.}\tau_H). \tag{13}$$

Here, h (respectively, H) denotes the maximum diameter of the elements in τ_h (resp. τ_H) and such that $h < H$. Let $X_h \subset X$, $M_h \subset M$ and $W_h \subset W$ be conforming finite element spaces, which defined as follows:

$$\begin{aligned}X_h &= \{v_h \in X \cap C^0(\Omega)^d\colon\ v_h|_K \in P_k(K)^d \quad \forall K \in \tau_h\},\\ M_h &= \{q_h \in M \cap C^0(\Omega)\colon\ q_h|_K \in P_s(K) \quad \forall K \in \tau_h\},\\ V_h &= \{v_h \in X_h\colon\ (q_h, \nabla\cdot v_h) = 0 \quad \forall q_h \in M_h\},\end{aligned} \tag{14}$$

where $P_r(K)$ is the space of the r-th order polynomial on K. The conforming velocity-pressure finite element space $(\mathbf{X}_\mathrm{h}, \mathrm{M}_\mathrm{h}) \subset (\mathbf{X}, \mathrm{M})$ satisfies the discrete inf-sup condition [2, 3], i.e., there exists a constant $\beta > 0$ independent of h such that

$$\inf_{q_h\in M_h}\sup_{v_h\in X_h} \frac{(q_h, \nabla\cdot v_h)}{\|q_h\|\|\nabla v_h\|} \ge \beta > 0. \tag{15}$$

As we know, this discrete inf-sup condition which are known to be valid for the classical Taylor-Hood element (P_k, P_{k-1}) [29], the (P_2, P_0) [30] element, and the Scott–Vogelius elements $(P_k, P_k^{\mathrm{disc}})$ on appropriate meshes [19].

The coarse or large scales space used in this article is defined by L_H, which is the coarse finite element spaces of the deformation tensor with

$$L_H \subseteq \nabla X_h \subset L := \left\{l_{ij} \in \left(L^2(\Omega)\right)^{d\times d} | l_{ij} = l_{ji}\right\}. \tag{16}$$

Suppose the finite element space pair (X_h, M_h) satisfies the following approximation properties [2, 31]:

$$\begin{aligned}\inf_{v_h\in X_h}\left\{\|u - v_h\|\right\} &\le Ch^{k+1}\|u\|_{k+1} \quad \forall u \in \left(H^{k+1}(\Omega)\right)^d \cap X,\\ \inf_{v_h\in X_h}\|u - v_h\|_1 &\le Ch^k\|u\|_{k+1} \quad \forall u \in \left(H^{k+1}(\Omega)\right)^d \cap X,\\ \inf_{q_h\in M_h}\|p - q_h\| &\le Ch^{s+1}\|p\|_{s+1} \quad \forall p \in H^k(\Omega) \cap M.\end{aligned} \tag{17}$$

Let Δt be the step size for t, $t_n = n\Delta t$, $n = 0, 1, 2, \ldots, N$, with $T := N\Delta t$. For notational clarity, let $v^{n+1/2} = v(t_{n+1/2})$ for the continuous variable, and $v_h^{n+1/2} = v_h^{n+1} + v_h^n/2$ for the discrete variable, here $t_{n+1/2} = (n + 1/2)\Delta t$, in addition, we define the following additional norms:

$$|||v|||_{\infty,k} := \max_{0\le n\le N-1}\left\|v^{n+1}\right\|_k, |||v|||_{m,k} := \left(\sum_{n=0}^{N-1}\left\|v^{n+1}\right\|_k^m \Delta t\right)^{1/m}. \tag{18}$$

The discrete Gronwall lemma plays an important role in the analysis, we recall from [28, 32] as follows:

Lemma 1 (Discrete Gronwall's lemma). *Let $\Delta t, H$, and a_n, b_n, c_n, d_n (for integers $n \geq 0$) be nonnegative numbers such that*

$$a_l + \Delta t \sum_{n=0}^{l} b_n \leq \Delta t \sum_{n=0}^{l-1} d_n a_n + \Delta t \sum_{n=0}^{l} c_n + H \quad \text{for } l \in \mathbb{N}. \tag{19}$$

Then, for all $\Delta t \geq 0$,

$$a_l + \Delta t \sum_{n=0}^{l} b_n \leq \exp\left(\Delta t \sum_{n=0}^{l-1} d_n\right)\left(\Delta t \sum_{n=0}^{l} c_n + H\right) \text{for } l \in \mathbb{N}. \tag{20}$$

Furthermore, Young's and Poincaré's inequalities as follows will be used frequently.

$$ab \leq \frac{\varepsilon}{p} a^p + \frac{\varepsilon^{-q/p}}{q} b^q, a, b, p, q, \varepsilon \in \mathbb{R}, \frac{1}{p} + \frac{1}{q} = 1, p, q \in (1, \infty), \varepsilon > 0,$$
$$\|v\| \leq C_p \|\nabla v\| \, \forall v \in X, C_p = C_p(\Omega). \tag{21}$$

Defining $P_{V_h}^{L^2} : L^2(\Omega) \longrightarrow V_h$ to be the L^2 projection into V_h, satisfying for $v \in L^2(\Omega)$

$$\left(P_{V_h}^{L^2} v - v, v_h\right) = 0, \quad \forall v_h \in V_h. \tag{22}$$

In the next lemma, we give out the important properties of the sparse-grad-div operator g [22]:

Lemma 2. *Let Ω be a bounded regular domain, and $u, v \in H^1(\Omega)^d$ ($d = 2$ or 3). Defining the sparse-grad-div operator g by*

$$g_{2d}(u, v) = \int_\Omega \left(u_{1x} v_{1x} + u_{2y} v_{2y} + 2u_{2y} v_{1x}\right) d\Omega,$$
$$g_{3d}(u, v) = \int_\Omega \left(u_{1x} v_{1x} + u_{2y} v_{2y} + u_{3z} v_{3z} + 2u_{2y} v_{1x} + 2u_{3z} v_{1x} + u_{3z} v_{2y} + u_{2y} v_{3z}\right) d\Omega. \tag{23}$$

Then, the operator g has the following properties:

(1) The operator g can be written as

$$g_{2d}(u, v) = (\nabla \cdot u, \nabla \cdot v) - \left((u_{1x}, v_{2x}) - (u_{2y}, v_{1x})\right),$$
$$g_{3d}(u, v) = (\nabla \cdot u, \nabla \cdot v) - \left((u_{1x}, v_{2x}) - (u_{2y}, v_{1x}) + (u_{1x}, v_{3z}) - (u_{3z}, v_{1x})\right). \tag{24}$$

(2) Similar to grad-div stabilization, g satisfies in $2d$ or $3d$, $g(u, u) = \|\nabla \cdot u\|^2$.

(3) If $\nabla \cdot u = 0$, then in $2d$ or $3d$, $g(u, v) = -(u_{1x}, \nabla \cdot v)$.

Now, we give out the subgrid-sparse-grad-div algorithm as follows:

Algorithm 3 (Subgrid-Sparse-Grad-Div). The full discrete approximation of (2) is: Let $u_h^{-1} = u_h^0 = P_{V_h}^{L^2} u_0$, given $u_h^{n-1}, u_h^n \in X_h, p_h^{n-1}, p_h^n \in M_h, G_H^n \in L_H$, find $u_h^{n+1} \in X_h, p_h^{n+1} \in M_h, G_H^{n+1} \in L_H$ satisfying, for $n = 0, 1, \ldots, N-1$

$$\begin{aligned}
&\left(\frac{u_h^{n+1}-u_h^n}{\Delta t}, v_h\right) + b^*\left(\frac{3}{2}u_h^n - \frac{1}{2}u_h^{n-1}, u_h^{n+1/2}, v_h\right) + (\nu+\alpha(h))\left(\nabla u_h^{n+1/2}, \nabla v_h\right) \\
&\quad - \alpha(h)\left(G_H^{n+1/2}, \nabla v_h\right) - \left(p_h^{n+1/2}, \nabla\cdot v_h\right) + \gamma g\left(u_h^{n+1/2}, v_h\right) \\
&\quad = \left(f\left(t_{n+1/2}\right), v_h\right), \quad \forall v_h \in X_h, \\
&\left(\nabla\cdot u_h^{n+1}, q_h\right) = 0, \quad \forall q_h \in M_h, \\
&\left(G_H^{n+1/2} - \nabla u_h^{n+1/2}, l_H\right) = 0, \quad \forall l_H \in L_H.
\end{aligned} \tag{25}$$

Remark 4. In Algorithm 3, we first add an artificial viscosity term on a fine scales, and then subtract it off only on the coarse scales, which leads to a much better conditioning of linear system is achieved while only altering the NS equations on fine scales. This allows us to solve incompressible flow problem with dominance of the convection, especially when the viscosity is too small.

Remark 5. We assume that $\alpha(h)$ is known, positive, element-wise constants. When $\alpha(h) \equiv 0$, Algorithm 3 become the Sparse-Grad-Div algorithm [22].

Remark 6. Combining the sparse-grad-div stabilization term with the pressure term, we can derive a modified pressure $P_h = p_h + \gamma(u_h)_{1_x}$, which will be used in the numerical experiments.

3. Stability Analysis

In this section, we establish the unconditional stability of Algorithm 3.

Theorem 7. *Assume that $f \in L^2(0,T;H^{-1}(\Omega))$, $u_0 \in L^2(\Omega)$, the solution of numerical scheme (25) satisfies the following energy estimates*

$$\left\|u_h^N\right\|^2 + \nu\Delta t\sum_{n=0}^{N-1}\left\|\nabla u_h^{n+1/2}\right\|^2 + 2\Delta t\gamma\sum_{n=0}^{N-1}\left\|\nabla\cdot u_h^{n+1/2}\right\|^2 \le \frac{1}{\gamma}\left\|\left|f_{1/2}\right\|\right|_{2,-1}^2 + \left\|u_h^0\right\|^2, \tag{26}$$

and

$$\nu\Delta t\sum_{n=0}^{N-1}\left\|G_H^{n+1/2}\right\|^2 \le \nu\Delta t\sum_{n=0}^{N-1}\left\|\nabla u_h^{n+1/2}\right\|^2 \le \frac{1}{\gamma}\left\|\left|f_{1/2}\right\|\right|_{2,-1}^2 + \left\|u_h^0\right\|^2. \tag{27}$$

Proof. Setting $l_H = G_H^{n+1/2}$ in the third equation of (25), then we obtain

$$\left\|G_H^{n+1/2}\right\|^2 = \left(\nabla u_h^{n+1/2}, G_H^{n+1/2}\right) \le \frac{1}{2}\left\|\nabla u_h^{n+1/2}\right\|^2 + \frac{1}{2}\left\|G_H^{n+1/2}\right\|^2, \tag{28}$$

which yields

$$\left\|G_H^{n+1/2}\right\| \le \left\|\nabla u_h^{n+1/2}\right\|. \tag{29}$$

Choosing $v_h = u_h^{n+1/2} \in V_h$ in (25), making use of Cauchy–Schwarz and Young's inequality to the right hand side, and thanks to Lemma 2, we arrive at

$$\begin{aligned}
&\frac{1}{2\Delta t}\left(\left\|u_h^{n+1}\right\|^2 - \left\|u_h^n\right\|^2\right) + (\nu+\alpha(h))\left\|\nabla u_h^{n+1/2}\right\|^2 + \gamma\left\|\nabla\cdot u_h^{n+1/2}\right\|^2 \\
&\le \alpha(h)\left\|G_H^{n+1/2}\right\|\left\|\nabla u_h^{n+1/2}\right\| + \frac{\nu}{2}\left\|\nabla u_h^{n+1/2}\right\|^2 + \frac{1}{2\nu}\left\|f\left(t_{n+1/2}\right)\right\|_{-1}^2.
\end{aligned} \tag{30}$$

Multiplying through by $2\Delta t$ and applying (29), it gives

$$\left\|u_h^{n+1}\right\|^2 - \left\|u_h^n\right\|^2 + \nu\Delta t\left\|\nabla u_h^{n+1/2}\right\|^2 + 2\Delta t\gamma\left\|\nabla\cdot u_h^{n+1/2}\right\|^2 \le \frac{\Delta t}{\nu}\left\|f\left(t_{n+1/2}\right)\right\|_{-1}^2. \tag{31}$$

Summing up from $n = 0$ to $N-1$, we obtain

$$\left\|u_h^N\right\|^2+\nu\Delta t\sum_{n=0}^{N-1}\left\|\nabla u_h^{n+1/2}\right\|^2+2\Delta t\gamma\sum_{n=0}^{N-1}\left\|\nabla\cdot u_h^{n+1/2}\right\|^2 \le\frac{\Delta t}{\nu}\sum_{n=0}^{N-1}\left\|f\left(t_{n+1/2}\right)\right\|_{-1}^2+\left\|u_h^0\right\|^2, \tag{32}$$

and then, we obtain the estimate (26). By (29) and (32), we get the bound of G_H as follows:

$$\nu\Delta t\sum_{n=0}^{N-1}\left\|G_H^{n+1/2}\right\|^2\le\nu\Delta t\sum_{n=0}^{N-1}\left\|\nabla u_h^{n+1/2}\right\|^2\le\frac{\Delta t}{\nu}\sum_{n=0}^{N-1}\left\|f\left(t_{n+1/2}\right)\right\|_{-1}^2+\left\|u_h^0\right\|^2, \tag{33}$$

which we get the bound (27), and complete the proof. □

4. Error Analysis

In this section, we devote to derive the error estimate of the presented numerical scheme (25). For convenience, we denote a generic constant C whose value may depends only on Ω and system parameters but is independent of the solutions, time step size and mesh width, and it may take on different value from place to place.

To establish the optimal asymptotic error estimate for the approximation, we assume that the true solution of problem (1) satisfies the following regularity assumptions:

$$\begin{aligned}&u\in L^\infty\left(0,T;H^1(\Omega)\right)\cap H^1\left(0,T;H^{k+1}(\Omega)\right)\cap H^3\left(0,T;L^2(\Omega)\right)\cap H^2\left(0,T;H^1(\Omega)\right),\\&p\in L^2\left(0,T;H^{s+1}(\Omega)\right).\end{aligned} \tag{34}$$

Theorem 8. *Let (u,p) be the solution of Navier–Stokes equations (1) and satisfy the regularity assumptions (18), (u_h^{n+1},p_h^{n+1}) is given by the scheme (10), then we have the following error estimate:*

$$\begin{aligned}&\left\|u(T)-u_h^N\right\|^2+\nu\Delta t\sum_{n=0}^{N-1}\left\|\nabla u\left(t_{n+\frac{1}{2}}\right)-\nabla u_h^{n+1/2}\right\|^2+\Delta t\gamma\sum_{n=0}^{N-1}\left\|\nabla\cdot u_h^{n+1/2}\right\|^2\\&\le C\Bigg(\nu h^{2k+2}|||u||_{2,k+1}^2+\frac{\alpha^2(h)}{\nu}h^{2k+2}|||u||_{2,k+1}^2+\frac{\gamma^2}{\nu}h^{2k}|||u||_{2,k+1}^2+\frac{1}{\nu}h^{2k}|||u||_{2,k+1}^2\\&\quad+\frac{\Delta t^4}{\nu}\left(|||u_{ttt}|||_{2,0}^2+|||u_{tt}|||_{4,0}^4\right)+\frac{\Delta t^4}{\nu}|||\nabla u||_{\infty,0}^4+\frac{\Delta t^4}{\nu}|||\nabla u_{1/2}|||_{\infty,0}^4\\&\quad+\frac{\Delta t^4}{\nu}|||\nabla u_{tt}|||_{4,0}^4+\nu\Delta t^4|||\nabla u_{tt}|||_{2,0}^2+\frac{h^{2k}}{\gamma}|||p-\gamma u_{1x}|||_{\infty,k}^2+\frac{\alpha^2(h)}{\nu}H^{2k}|||u||_{2,k+1}^2\Bigg).\end{aligned} \tag{35}$$

Remark 9. From the right hand side of estimate (19), we can see that the sparse-grad-div operator g act to reduce the effect of pressure discretization error on the velocity error and increase the effect of the velocity discretization error.

Proof. We rewrite the continuous variational formulations of equation (2) at $t = t_{n+1}$. For $v_h \in V_h$, adding and subtracting some terms yield

$$\begin{aligned}
&\left(\frac{u(t_{n+1})-u(t_n)}{\Delta t}, v_h\right) + b^*\left(\frac{3}{2}u(t_n) - \frac{1}{2}u(t_{n-1}), \frac{u(t_{n+1})+u(t_n)}{2}, v_h\right) + \nu\left(\frac{u(t_{n+1})+u(t_n)}{2}, \nabla v_h\right) \\
&\quad + \alpha(h)\left(\frac{u(t_{n+1})+u(t_n)}{2}, \nabla v_h\right) - \left(p(t_{n+1/2}), \nabla\cdot v_h\right) + \gamma g\left(\frac{u(t_{n+1})+u(t_n)}{2}, v_h\right) \\
&= \left(\frac{u(t_{n+1})-u(t_n)}{\Delta t} - u_t(t_{n+1/2}), v_h\right) + b^*\left(\frac{3}{2}u(t_n) - \frac{1}{2}u(t_{n-1}), \frac{u(t_{n+1})+u(t_n)}{2}, v_h\right) \\
&\quad - b^*\left(u(t_{n+1/2}), u(t_{n+1/2}), v_h\right) + \nu\left(\nabla\frac{u(t_{n+1})+u(t_n)}{2} - \nabla u(t_{n+1/2}), v_h\right) \\
&\quad + \alpha(h)\left(\nabla\frac{u(t_{n+1})+u(t_n)}{2}, \nabla v_h\right) - \gamma\left(u_{1x}^{n+1/2}, \nabla\cdot v_h\right) + \left(f(t_{n+1/2}), v_h\right).
\end{aligned} \tag{36}$$

Denoting by $e^n = u(t_n) - u_h^n$, after subtracting (25) from (36) and performing some simple algebraic manipulations, we obtained the error equation as follows

$$\begin{aligned}
&\left(\frac{e^{n+1}-e^n}{\Delta t}, v_h\right) + \nu\left(\nabla e^{n+1/2}, \nabla v_h\right) + \alpha(h)\left(\nabla e^{n+1/2}, \nabla v_h\right) + \gamma g\left(e^{n+1/2}, v_h\right) \\
&= -b^*\left(\frac{3}{2}e^n - \frac{1}{2}e^{n-1}, \frac{u(t_{n+1})+u(t_n)}{2}, v_h\right) - b^*\left(\frac{3}{2}u_h^n - \frac{1}{2}u_h^{n-1}, e^{n+1/2}, v_h\right) \\
&\quad + \left(\frac{u(t_{n+1})-u(t_n)}{\Delta t} - u_t(t_{n+1/2}), v_h\right) + \nu\left(\nabla\frac{u(t_{n+1})+u(t_n)}{2} - \nabla u(t_{n+1/2}), v_h\right) \\
&\quad + b^*\left(\frac{3}{2}u(t_n) - \frac{1}{2}u(t_{n-1}), \frac{u(t_{n+1})+u(t_n)}{2}, v_h\right) - b^*\left(u(t_{n+1/2}), u(t_{n+1/2}), v_h\right) \\
&\quad + \alpha(h)\left(\nabla\frac{u(t_{n+1})+u(t_n)}{2} - G_H^{n+1/2}, \nabla v_h\right) + \gamma\left(p(t_{n+1/2}) - u_{1x}^{n+1/2} - q_h, \nabla\cdot v_h\right).
\end{aligned} \tag{37}$$

Next, we decompose the errors into interpolation error and approximation error terms as follows:

$$e^n = \left(u(t_n) - P_{V_h}^{L^2} u(t_n)\right) - \left(u_h^n - P_{V_h}^{L^2} u(t_n)\right) = \eta^n - \phi_h^n, \tag{38}$$

and rewrite (37) as follows:

$$\begin{aligned}
&\frac{1}{\Delta t}\left(\phi_h^{n+1} - \phi_h^n, v_h\right) + \nu\left(\nabla\phi_h^{n+1/2}, \nabla v_h\right) + \alpha(h)\left(\nabla\phi_h^{n+1/2}, \nabla v_h\right) + \gamma g\left(\phi_h^{n+1/2}, v_h\right) \\
&= \frac{1}{\Delta t}\left(\eta^{n+1} - \eta^n, v_h\right) + \nu\left(\nabla\eta^{n+1/2}, \nabla v_h\right) + \alpha(h)\left(\nabla\eta^{n+1/2}, \nabla v_h\right) + \gamma g\left(\eta^{n+1/2}, v_h\right) \\
&\quad + b^*\left(\frac{3}{2}\eta^n - \frac{1}{2}\eta^{n-1}, \frac{u(t_{n+1}) + u(t_n)}{2}, v_h\right) - b^*\left(\frac{3}{2}\phi_h^n - \frac{1}{2}\phi_h^{n-1}, \frac{u(t_{n+1}) + u(t_n)}{2}, v_h\right) \\
&\quad + b^*\left(\frac{3}{2}u_h^n - \frac{1}{2}u_h^{n-1}, \eta^{n+1/2}, v_h\right) - b^*\left(\frac{3}{2}u_h^n - \frac{1}{2}u_h^{n-1}, \phi_h^{n+1/2}, v_h\right) \\
&\quad - \left(\frac{u(t_{n+1}) - u(t_n)}{\Delta t} - u_t(t_{n+1/2}), v_h\right) - b^*\left(\frac{3}{2}u(t_n) - \frac{1}{2}u(t_{n-1}), \frac{u(t_{n+1}) + u(t_n)}{2} - u(t_{n+1/2}), v_h\right) \\
&\quad - b^*\left(\frac{3}{2}u(t_n) - \frac{1}{2}u(t_{n-1}) - u(t_{n+1/2}), u(t_{n+1/2}), v_h\right) - \nu\left(\nabla\frac{u(t_{n+1}) + u(t_n)}{2} - \nabla u(t_{n+1/2}), v_h\right) \\
&\quad - \alpha(h)\left(\nabla\frac{u(t_{n+1}) + u(t_n)}{2} - G_H^{n+1/2}, \nabla v_h\right) - \gamma\left(p(t_{n+1/2}) - u_{1x}^{n+1/2} - q_h, \nabla\cdot v_h\right),
\end{aligned} \tag{39}$$

for all $q_h \in M_h$.

Setting $v_h = \phi_h^{n+1/2} \in V_h$ in (39) and using Lemma 2, we arrived at

$$
\begin{aligned}
&\frac{1}{2\Delta t}\left(\left\|\phi_h^{n+1}\right\|^2-\left\|\phi_h^{n}\right\|^2\right)+\nu\left\|\nabla\phi_h^{n+1/2}\right\|^2+\alpha(h)\left\|\nabla\phi_h^{n+1/2}\right\|^2+\gamma\left\|\nabla\cdot\phi_h^{n+1/2}\right\|^2\\
&=\frac{1}{\Delta t}\left(\eta^{n+1}-\eta^{n},\phi_h^{n+1/2}\right)+\nu\left(\nabla\eta^{n+1/2},\nabla\phi_h^{n+1/2}\right)+\alpha(h)\left(\nabla\eta^{n+1/2},\nabla\phi_h^{n+1/2}\right)+\gamma g\left(\eta^{n+1/2},\phi_h^{n+1/2}\right)\\
&\quad+b^*\left(\frac{3}{2}\eta^{n}-\frac{1}{2}\eta^{n-1},\frac{u(t_{n+1})+u(t_n)}{2},\phi_h^{n+1/2}\right)-b^*\left(\frac{3}{2}\phi_h^{n}-\frac{1}{2}\phi_h^{n-1},\frac{u(t_{n+1})+u(t_n)}{2},\phi_h^{n+1/2}\right)\\
&\quad+b^*\left(\frac{3}{2}u_h^{n}-\frac{1}{2}u_h^{n-1},\eta^{n+1/2},\phi_h^{n+1/2}\right)-b^*\left(\frac{3}{2}u_h^{n}-\frac{1}{2}u_h^{n-1},\phi_h^{n+1/2},\phi_h^{n+1/2}\right)\\
&\quad-\left(\frac{u(t_{n+1})-u(t_n)}{\Delta t}-u_t\left(t_{n+\frac{1}{2}}\right),\phi_h^{n+1/2}\right)\\
&\quad-b^*\left(\frac{3}{2}u(t_n)-\frac{1}{2}u(t_{n-1})-u\left(t_{n+\frac{1}{2}}\right),u\left(t_{n+\frac{1}{2}}\right),\phi_h^{n+1/2}\right)\\
&\quad-b^*\left(\frac{3}{2}u(t_n)-\frac{1}{2}u(t_{n-1}),\frac{u(t_{n+1})+u(t_n)}{2}-u(t_{n+1/2}),\phi_h^{n+1/2}\right)\\
&\quad-\nu\left(\nabla\frac{u(t_{n+1})+u(t_n)}{2}-\nabla u(t_{n+1/2}),\nabla\phi_h^{n+1/2}\right)\\
&\quad-\alpha(h)\left(\nabla\frac{u(t_{n+1})+u(t_n)}{2}-G_H^{n+1/2},\nabla\phi_h^{n+1/2}\right)\\
&\quad-\left(p(t_{n+1/2})-\gamma u_{1x}^{n+1/2}-q_h,\nabla\cdot\phi_h^{n+1/2}\right).
\end{aligned}
\tag{40}
$$

Due to the orthogonality of L^2 projection operator $P_{V_h}^{L^2}$, that $\eta^{n+1}-\eta^{n}\perp V_h$, so $1/\Delta t(\eta^{n+1}-\eta^{n},\phi_h^{n+1})=0$. Using the property (9) of the trilinear b, which implies $b^*(3/2u_h^{n}-1/2u_h^{n-1},\phi_h^{n+1/2},\phi_h^{n+1/2})=0$. Next, we estimate the rest terms on the RHS of (40) one by one. First, the applications of Cauchy–Schwarz and Young's inequality lead to

$$
\nu\left(\nabla\eta_h^{n+1/2},\nabla\phi_h^{n+1/2}\right)\le\frac{\nu}{28}\left\|\nabla\phi_h^{n+1/2}\right\|^2+C\nu\left\|\nabla\eta^{n+1/2}\right\|^2,
\tag{41}
$$

and

$$
\alpha(h)\left(\nabla\eta_h^{n+1/2},\nabla\phi_h^{n+1/2}\right)\le\frac{\nu}{28}\left\|\nabla\phi_h^{n+1/2}\right\|^2+\frac{C\alpha^2(h)}{\nu}\left\|\nabla\eta^{n+1/2}\right\|^2,
\tag{42}
$$

also

$$
\gamma g\left(\eta_h^{n+1/2},\phi_h^{n+1/2}\right)\le C\gamma\left\|\nabla\eta_h^{n+1/2}\right\|\left\|\nabla\phi_h^{n+1/2}\right\|\le\frac{\nu}{28}\left\|\nabla\phi_h^{n+1/2}\right\|^2+\frac{C\gamma^2}{\nu}\left\|\nabla\eta^{n+1/2}\right\|^2.
\tag{43}
$$

For the nonlinear term, using estimates (10) and (12), it gives

$$
\begin{aligned}
&b^*\left(\frac{3}{2}\eta^{n}-\frac{1}{2}\eta^{n-1},\frac{u(t_{n+1})+u(t_n)}{2},\phi_h^{n+1/2}\right)\\
&\le C\left\|\nabla\left(\frac{3}{2}\eta^{n}-\frac{1}{2}\eta^{n-1}\right)\right\|\left\|\nabla\frac{u(t_{n+1})+u(t_n)}{2}\right\|\left\|\nabla\phi_h^{n+1/2}\right\|\\
&\le\frac{\nu}{28}\left\|\nabla\phi_h^{n+1/2}\right\|^2+\frac{C}{\nu}\left(\left\|\nabla u(t_{n+1})\right\|^2+\left\|\nabla u(t_n)\right\|^2\right)\left(\left\|\nabla\eta^{n}\right\|^2+\left\|\nabla\eta^{n-1}\right\|^2\right),
\end{aligned}
\tag{44}
$$

and

$$\begin{aligned}
&b^*\left(\frac{3}{2}\phi_h^n-\frac{1}{2}\phi_h^{n-1},\frac{u(t_{n+1})+u(t_n)}{2},\phi_h^{n+1/2}\right)\\
&\le C\left\|\frac{3}{2}\phi_h^n-\frac{1}{2}\phi_h^{n-1}\right\|\left(\left\|\frac{u(t_{n+1})+u(t_n)}{2}\right\|_\infty+\left\|\nabla\frac{u(t_{n+1})+u(t_n)}{2}\right\|_\infty\right)\|\nabla\phi_h^{n+1/2}\|\\
&\le\frac{\nu}{28}\|\nabla\phi_h^{n+1/2}\|^2+\frac{C}{\nu}\left(\|u(t_{n+1})+u(t_n)\|_\infty^2+\|\nabla(u(t_{n+1})+u(t_n))\|_\infty^2\right)\left(\|\phi_h^n\|^2+\|\phi_h^{n-1}\|^2\right),
\end{aligned}\tag{45}$$

For the next nonlinear term, we have the identity

$$\begin{aligned}
&b^*\left(\frac{3}{2}u_h^n-\frac{1}{2}u_h^{n-1},\eta^{n+1/2},\phi_h^{n+1/2}\right)\\
&=b^*\left(\frac{3}{2}u(t_n)-\frac{1}{2}u(t_{n-1}),\eta^{n+1/2},\phi_h^{n+1/2}\right)-b^*\left(\frac{3}{2}\eta^n-\frac{1}{2}\eta^{n-1},\eta^{n+1/2},\phi_h^{n+1/2}\right)\\
&\quad+b^*\left(\frac{3}{2}\phi_h^n-\frac{1}{2}\phi_h^{n-1},\eta^{n+1/2},\phi_h^{n+1/2}\right).
\end{aligned}\tag{46}$$

The right hand side of (46) can be bounded as follows. First,

$$\begin{aligned}
&b^*\left(\frac{3}{2}u(t_n)-\frac{1}{2}u(t_{n-1}),\eta^{n+1/2},\phi_h^{n+1/2}\right)\\
&\le\frac{\nu}{28}\|\nabla\phi_h^{n+1/2}\|^2+\frac{C}{\nu}\left(\|\nabla u(t_n)\|^2+\|\nabla u(t_{n-1})\|^2\right)\|\nabla\eta^{n+1/2}\|^2.
\end{aligned}\tag{47}$$

Next,

$$\begin{aligned}
&b^*\left(\frac{3}{2}\eta^n-\frac{1}{2}\eta^{n-1},\eta^{n+1/2},\phi_h^{n+1/2}\right)\\
&\le\frac{\nu}{28}\|\nabla\phi_h^{n+1/2}\|^2+\frac{C}{\nu}\left(\|\nabla\eta^n\|^2+\|\nabla\eta^{n-1}\|^2\right)\|\nabla\eta^{n+1/2}\|^2.
\end{aligned}\tag{48}$$

The last term in (46) can be bounded as

$$\begin{aligned}
&b^*\left(\frac{3}{2}\phi_h^n-\frac{1}{2}\phi_h^{n-1},\eta^{n+1/2},\phi_h^{n+1/2}\right)\\
&\le C\sqrt{\left\|\frac{3}{2}\phi_h^n-\frac{1}{2}\phi_h^{n-1}\right\|\left\|\frac{3}{2}\nabla\phi_h^n-\frac{1}{2}\nabla\phi_h^{n-1}\right\|}\|\nabla\eta^{n+1/2}\|\|\nabla\phi_h^{n+1/2}\|\\
&\le\frac{\nu}{28}\|\nabla\phi_h^{n+1/2}\|^2+\frac{C}{\nu}\left\|\frac{3}{2}\phi_h^n-\frac{1}{2}\phi_h^{n-1}\right\|\left\|\frac{3}{2}\nabla\phi_h^n-\frac{1}{2}\nabla\phi_h^{n-1}\right\|\|\nabla\eta^{n+1/2}\|\\
&\le\frac{\nu}{28}\|\nabla\phi_h^{n+1/2}\|^2+\frac{C}{\nu}\|\phi_h^n+\phi_h^{n-1}\|\|\nabla\phi_h^n+\nabla\phi_h^{n-1}\|\|\nabla\eta^{n+1/2}\|\\
&\le\frac{\nu}{28}\|\nabla\phi_h^{n+1/2}\|^2+\frac{Ch^{-1}}{\nu}\|\phi_h^n+\phi_h^{n-1}\|\|\nabla\eta^{n+1/2}\|.
\end{aligned}\tag{49}$$

Combining estimates (47)–(49), we can get the bound of the RHS of (46). The rest of terms of (40) can be estimated as follows:

$$\begin{aligned}
&\left(\frac{u(t_{n+1})-u(t_n)}{\Delta t}-u_t(t_{n+1/2}),\phi_h^{n+1/2}\right)\\
&\le C\left\|\frac{u(t_{n+1})-u(t_n)}{\Delta t}-u_t(t_{n+1/2})\right\|\|\nabla\phi_h^{n+1/2}\|\\
&\le\frac{\nu}{28}\|\nabla\phi_h^{n+1/2}\|^2+\frac{C}{\nu}\Delta t^3\int_{t_n}^{t_{n+1}}\|u_{\mathrm{ttt}}\|^2dt,
\end{aligned}\tag{50}$$

and

$$\begin{aligned}
&b^*\left(\frac{3}{2}u(t_n)-\frac{1}{2}u(t_{n-1}),\frac{u(t_{n+1})+u(t_n)}{2}-u(t_{n+1/2}),\phi_h^{n+1/2}\right)\\
&\le C\left\|\frac{3}{2}\nabla u(t_n)-\frac{1}{2}\nabla u(t_{n-1})\right\|\left\|\nabla\frac{u(t_{n+1})+u(t_n)}{2}-\nabla u(t_{n+1/2})\right\|\|\nabla\phi_h^{n+1/2}\|\\
&\le\frac{\nu}{28}\|\nabla\phi_h^{n+1/2}\|^2+\frac{C}{\nu}\Delta t^3\left(\|\nabla u(t_n)\|^2+\|\nabla u(t_{n-1})\|^2\right)\int_{t_n}^{t_{n+1}}\|\nabla u_{tt}\|^2dt\\
&\le\frac{\nu}{28}\left\|\nabla\phi_h^{n+\frac{1}{2}}\right\|^2+\frac{C}{\nu}\Delta t^4\left(\|\nabla u(t_n)\|^4+\|\nabla u(t_{n-1})\|^4\right)+\frac{C}{\nu}\Delta t^3\int_{t_n}^{t_{n+1}}\|\nabla u_{tt}\|^4dt,
\end{aligned}\tag{51}$$

and

$$\begin{aligned}
&b^*\left(\frac{3}{2}u(t_n)-\frac{1}{2}u(t_{n-1})-u(t_{n+1/2}),u(t_{n+1/2}),\phi_h^{n+1/2}\right)\\
&\le C\left\|\nabla\left(\frac{3}{2}u(t_n)-\frac{1}{2}u(t_{n-1})-u(t_{n+1/2})\right)\right\|\|\nabla u(t_{n+1/2})\|\|\nabla\phi_h^{n+1/2}\|\\
&\le\frac{\nu}{28}\|\nabla\phi_h^{n+1/2}\|^2+\frac{C}{\nu}\left\|\nabla\left(\frac{3}{2}u(t_n)-\frac{1}{2}u(t_{n-1})-u(t_{n+1/2})\right)\right\|\|\nabla u(t_{n+1/2})\|\\
&\le\frac{\nu}{28}\|\nabla\phi_h^{n+1/2}\|^2+\frac{C}{\nu}\Delta t^3\|\nabla u(t_{n+1/2})\|^2\int_{t_n}^{t_{n+1}}\|\nabla u_{tt}\|^2dt\\
&\le\frac{\nu}{28}\|\nabla\phi_h^{n+1/2}\|^2+\frac{C}{\nu}\Delta t^4\|\nabla u(t_{n+1/2})\|^4+\frac{C}{\nu}\Delta t^3\int_{t_n}^{t_{n+1}}\|\nabla u_{tt}\|^4dt,
\end{aligned}\tag{52}$$

and

$$\begin{aligned}
&\nu\left(\nabla\frac{u(t_{n+1})+u(t_n)}{2}-\nabla u(t_{n+1/2}),\nabla\phi_h^{n+1/2}\right)\\
&\le C\left\|\nabla\frac{u(t_{n+1})+u(t_n)}{2}-\nabla u(t_{n+1/2})\right\|\|\nabla\phi_h^{n+1/2}\|\\
&\le\frac{\nu}{28}\|\nabla\phi_h^{n+1/2}\|^2+C\nu\Delta t^3\int_{t_n}^{t_{n+1}}\|\nabla u_{tt}\|^2dt.
\end{aligned}\tag{53}$$

For the pressure term, we have

$$\begin{aligned}
&\left(p(t_{n+1/2})-\gamma u_{1x}^{n+1/2}-q_h,\nabla\cdot\phi_h^{n+1/2}\right)\\
&\le\|p(t_{n+1/2})-\gamma u_{1x}^{n+1/2}-q_h\|\|\nabla\cdot\phi_h^{n+1/2}\|\\
&\le\frac{\gamma}{2}\|\nabla\cdot\phi_h^{n+1/2}\|^2+\frac{C}{\gamma}\|p(t_{n+1/2})-\gamma u_{1x}^{n+1/2}-q_h\|^2dt.
\end{aligned}\tag{54}$$

Finally, we estimate the coarse mesh projection term, by the third equation of (25), we know for $l_H\in L_H$

$$\begin{aligned}&\left(\nabla\frac{u(t_{n+1})+u(t_n)}{2}-G_H^{n+1/2},l_H\right)\\&=\left(\nabla\frac{u(t_{n+1})+u(t_n)}{2}-\nabla u_h^{n+1/2},l_H\right)\\&=\left(\nabla e^{n+1/2},l_H\right).\end{aligned}\tag{55}$$

We denote $\Psi^n=\nabla u^n-P_{L_H}^{L^2}(\nabla u^n)$, $\Upsilon_H^n=G_H^n-P_{L_H}^{L^2}(\nabla u^n)$; here, $P_{L_H}^{L^2}$ is L^2 projection onto L_H. Thanks to the orthogonality of L^2 projection operator $P_{L_H}^{L^2}$, that $\Psi^n\perp L_H$, so

$$\begin{aligned}\left(\nabla e^{n+1/2},l_H\right)&=\left(\nabla\frac{u(t_{n+1})+u(t_n)}{2}-G_H^{n+1/2},l_H\right)\\&=\left(\Psi^{n+1/2},l_H\right)-\left(\Upsilon_h^{n+1/2},l_H\right)\\&=-\left(\Upsilon_h^{n+1/2},l_H\right).\end{aligned}\tag{56}$$

Choosing $l_H=\Upsilon_h^{n+1/2}$ in above equation, it gives

$$\begin{aligned}\left\|\Upsilon_h^{n+1/2}\right\|^2&=-\left(\nabla e^{n+1/2},\Upsilon_h^{n+1/2}\right)\\&\le\left\|\nabla e^{n+1/2}\right\|\left\|\Upsilon_h^{n+1/2}\right\|\\&\le\frac{1}{2}\left\|\nabla e^{n+1/2}\right\|^2+\frac{1}{2}\left\|\Upsilon_h^{n+1/2}\right\|^2,\end{aligned}\tag{57}$$

which yields

$$\left\|\Upsilon_h^{n+1/2}\right\|\le\left\|\nabla e^{n+1/2}\right\|\le\left\|\nabla\eta^{n+1/2}\right\|+\left\|\nabla\phi_h^{n+1/2}\right\|,\tag{58}$$

and

$$\begin{aligned}&\alpha(h)\left(\nabla\frac{u(t_{n+1})+u(t_n)}{2}-G_H^{n+1/2},\nabla\phi_h^{n+1/2}\right)\\&\le\alpha(h)\left\|\Psi^{n+1/2}+\Upsilon_h^{n+1/2}\right\|\left\|\nabla\phi_h^{n+1/2}\right\|\\&\le\alpha(h)\left(\left\|\Psi^{n+1/2}\right\|+\left\|\Upsilon_h^{n+1/2}\right\|\right)\left\|\nabla\phi_h^{n+1/2}\right\|\\&\le\alpha(h)\left(\left\|\Psi^{n+1/2}\right\|+\left\|\nabla\eta^{n+1/2}\right\|+\left\|\nabla\phi_h^{n+1/2}\right\|\right)\left\|\nabla\phi_h^{n+1/2}\right\|\\&\le\alpha(h)\left\|\nabla\phi_h^{n+1/2}\right\|^2+\frac{\nu}{14}\left\|\nabla\phi_h^{n+1/2}\right\|^2+\frac{C\alpha^2(h)}{\nu}\left\|\Psi^{n+1/2}\right\|^2+\frac{C\alpha^2(h)}{\nu}\left\|\nabla\eta^{n+1/2}\right\|^2.\end{aligned}\tag{59}$$

After inserting the bound (41)–(59) into (40), multiplying by $2\Delta t$ on both side, and taking the sum from $n=1$ to $N-1$, noting that $\phi_h^0=0$, we have

$$
\begin{aligned}
&\left\|\phi_h^N\right\|^2+\nu\Delta t\sum_{n=0}^{N-1}\left\|\nabla\phi_h^{n+1/2}\right\|^2+\Delta t\gamma\sum_{n=0}^{N-1}\left\|\nabla\cdot\phi_h^{n+1/2}\right\|^2\\
&\le C\Delta t\sum_{n=0}^{N-1}\Big[\nu\left\|\eta^{n+1/2}\right\|^2+\frac{\alpha^2(h)}{\nu}\left\|\nabla\eta^{n+1/2}\right\|^2+\frac{\gamma^2}{\nu}\left\|\nabla\eta^{n+1/2}\right\|^2\\
&\quad+\frac{1}{\nu}\left(\left\|\nabla u(t_{n+1})\right\|^2+\left\|\nabla u(t_n)\right\|^2\right)\left(\left\|\nabla\eta^n\right\|^2+\left\|\nabla\eta^{n-1}\right\|^2\right)\\
&\quad+\frac{1}{\nu}\left(\left\|\nabla u(t_n)\right\|^2+\left\|\nabla u(t_{n-1})\right\|^2\right)\left\|\nabla\eta^{n+1/2}\right\|^2\\
&\quad+\frac{1}{\nu}\left(\left\|\nabla\eta^n\right\|^2+\left\|\nabla\eta^{n-1}\right\|^2\right)\left\|\nabla\eta^{n+1/2}\right\|^2+\frac{\Delta t^3}{\nu}\int_{t_n}^{t_{n+1}}\left\|u_{ttt}\right\|^2dt\\
&\quad+\frac{\Delta t^4}{\nu}\left(\left\|\nabla u(t_n)\right\|^4+\left\|\nabla u(t_{n-1})\right\|^4\right)+\frac{\Delta t^3}{\nu}\int_{t_n}^{t_{n+1}}\left\|\nabla u_{tt}\right\|^4dt\\
&\quad+\frac{\Delta t^4}{\nu}\left\|\nabla u(t_{n+1/2})\right\|^4+\nu\Delta t^3\int_{t_n}^{t_{n+1}}\left\|\nabla u_{tt}\right\|^2dt+\frac{1}{\gamma}\inf_{q_h\in M_h}\left\|p(t_{n+1/2})-\gamma u_{1x}^{n+1/2}-q_h\right\|^2dt\\
&\quad+\frac{\alpha^2(h)}{\nu}\inf_{l_h\in L_H}\left\|\nabla u^{n+1/2}-l_H\right\|^2\\
&\quad+\frac{1}{\nu}\left(\left\|u(t_{n+1})+u(t_n)\right\|_\infty^2+\left\|\nabla(u(t_{n+1})+u(t_n))\right\|_\infty^2\right)\left(\left\|\phi_h^n\right\|^2+\left\|\phi_h^{n-1}\right\|^2\right)\\
&\quad+\frac{h^{-1}}{\nu}\left\|\phi_h^n+\phi_h^{n-1}\right\|\left\|\nabla\eta^{n+1/2}\right\|\Big].
\end{aligned}
\tag{60}
$$

Absorbing constants into C, it gives

$$
\begin{aligned}
&\left\|\phi_h^N\right\|^2+\nu\Delta t\sum_{n=0}^{N-1}\left\|\nabla\phi_h^{n+1/2}\right\|^2+\Delta t\gamma\sum_{n=0}^{N-1}\left\|\nabla\cdot\phi_h^{n+1/2}\right\|^2\\
&\le C\Bigg(\nu h^{2k+2}\|\,|u|\,\|_{2,k+1}^2+\frac{\alpha^2(h)}{\nu}h^{2k}\|\,|u|\,\|_{2,k+1}^2+\frac{\gamma^2}{\nu}h^{2k}\|\,|u|\,\|_{2,k+1}^2+\frac{1}{\nu}h^{2k}\|\,|u|\,\|_{2,k+1}^2\\
&\quad+\frac{\Delta t^4}{\nu}\left(\left\|\,|u_{ttt}|\,\right\|_{2,0}^2+\left\|\,|u_{tt}|\,\right\|_{4,0}^4\right)+\frac{\Delta t^4}{\nu}\|\,|\nabla u|\,\|_{\infty,0}^4+\frac{\Delta t^4}{\nu}\left\|\,|\nabla u_{1/2}|\,\right\|_{\infty,0}^4\\
&\quad+\frac{\Delta t^4}{\nu}\left\|\,|\nabla u_{tt}|\,\right\|_{4,0}^4+\nu\Delta t^4\left\|\,|\nabla u_{tt}|\,\right\|_{2,0}^2+\frac{h^{2k}}{\gamma}\left\|\,|p-\gamma u_{1x}|\,\right\|_{\infty,k}^2+\frac{\alpha^2(h)}{\nu}H^{2k}\|\,|u|\,\|_{2,k+1}^2\Bigg)\\
&\quad+\left(C\frac{\Delta t}{\nu}+\frac{1}{\nu}h^{2k-1}\Delta t\|\,|u|\,\|_{\infty,k+1}^2\right)\sum_{n=0}^{N-1}\left\|\phi_h^n\right\|^2.
\end{aligned}
\tag{61}
$$

Hence, with $0<\Delta t,h<1$, from the discrete Gronwall lemma yields

$$\begin{aligned}
&\left\|\phi_h^N\right\|^2+\nu\Delta t\sum_{n=0}^{N-1}\left\|\nabla\phi_h^{n+1/2}\right\|^2+\Delta t\gamma\sum_{n=0}^{N-1}\left\|\nabla\cdot\phi_h^{n+1/2}\right\|^2\\
&\le C\Bigg(\nu h^{2k+2}|||u|||_{2,k+1}^2+\frac{\alpha^2(h)}{\nu}h^{2k}|||u|||_{2,k+1}^2+\frac{\gamma^2}{\nu}h^{2k}|||u|||_{2,k+1}^2+\frac{1}{\nu}h^{2k}|||u|||_{2,k+1}^2\\
&\quad+\frac{\Delta t^4}{\nu}\left(\left|\left|\left|u_{ttt}\right|\right|\right|_{2,0}^2+\left|\left|\left|u_{tt}\right|\right|\right|_{4,0}^4\right)+\frac{\Delta t^4}{\nu}|||\nabla u|||_{\infty,0}^4+\frac{\Delta t^4}{\nu}\left|\left|\left|\nabla u_{1/2}\right|\right|\right|_{\infty,0}^4\\
&\quad+\frac{\Delta t^4}{\nu}\left|\left|\left|\nabla u_{tt}\right|\right|\right|_{4,0}^4+\nu\Delta t^4\left|\left|\left|\nabla u_{tt}\right|\right|\right|_{2,0}^2+\frac{h^{2k}}{\gamma}\left|\left|\left|p-\gamma u_{1x}\right|\right|\right|_{\infty,k}^2+\frac{\alpha^2(h)}{\nu}H^{2k}|||u|||_{2,k+1}^2\Bigg).
\end{aligned}\tag{62}$$

By applying the triangle inequality, we obtain the error estimate (35). □

Corollary 10. *Consider the numerical method (10), under the assumptions of Theorem 8, with (X_h, M_h) given by the Taylor-Hood approximation element $(k = 2, s = 1)$, and choose $L_H = P_1(\tau_H)$, then there exist a positive constant C such that*

$$\begin{aligned}
&\left\|u(T)-u_h^N\right\|^2+\nu\Delta t\sum_{n=0}^{N-1}\left\|\nabla u\left(t_{n+1/2}\right)-\nabla u_h^{n+1/2}\right\|^2+\Delta t\gamma\sum_{n=0}^{N-1}\left\|\nabla\cdot u_h^{n+1/2}\right\|^2\\
&\le C\left(\Delta t^4+h^4+\alpha^2(h)H^4\right).
\end{aligned}\tag{63}$$

5. Numerical Experiments

Herein, we perform some numerical experiments to test the effectiveness of the presented method. We choose $P_2 - P_1$ finite element pair to approximate the velocity and pressure. The domain Ω is subdivided into triangles. All the numerics were implemented by using the public domain finite element software package Freefem++ [33].

There are two test problems are performed. First, we perform a problem with known analytical solution to validate the convergence rates of Algorithm 3. The next experiment is for simulating the benchmark problem of flow around a cylinder [34, 35]. In all cases, the proposed methods perform very effectively.

5.1. Convergence Rate Verification. Our first example is designed to verify the predicted convergence rates of Algorithm 3. The problem is an interesting test problem for simulating decay of Green–Taylor vortex [36–38], which has following the analytic solution.

$$\begin{aligned}
u_1(x,y,t)&=-\cos(n\pi x)\sin(n\pi y)\exp\left(-2n^2\pi^2\nu t\right),\\
u_2(x,y,t)&=\sin(n\pi x)\cos(n\pi y)\exp\left(-2n^2\pi^2\nu t\right),\\
p(x,y,t)&=-\frac{1}{4}(\cos(2n\pi x)+\cos(2n\pi y))\exp\left(-2n^2\pi^2\nu t\right).
\end{aligned}\tag{64}$$

This is a solution of the NSE with $f = 0$, consisting of an $n \times n$ array of oppositely signed vortices that decay in time. The initial condition at $t = 0$ is above true solution. We consider the convergence rates of Algorithm 3 to this solution on the domain $\Omega = (0, 1) \times (0, 1)$ and time interval $[0, T]$. Taking $n = 1$, $\alpha(h) = h$, $\gamma = 1$, final time $T = 1$, and setting the values of the time step size Δt and the mesh width h so that for a refinement, each of Δt and h gets cut in a half. We choose Re = 100,1000 and 10000. The convergence rates are calculated from the errors at two successive values of h in the usual manner by postulating $E(h) = Ch^r$ and solving the formula.

$$r=\frac{\log\left(E(h_i)/E(h_{i+1})\right)}{\log\left(h_i/h_{i+1}\right)},\tag{65}$$

where $E(h_i)$ and $E(h_{i+1})$ are the errors corresponding to the mesh size h_i and h_{i+1}, respectively. The results are shown in Tables 1–3. We can see from that, the proposed Subgrid-Sparse-Div-Grad stabilization method can keep the rates of convergence excellently for different Re values, which are in good agreement with the theoretical convergence rates predictions.

5.2. Flow around a Cylinder. The second example is the two-dimensional flow around a cylinder, which is a popular benchmark problem for testing numerical schemes of time-dependent Navier–Stokes equations. The domain $\Omega = [0, 2.2] \times [0, 0.41]$ contains a cylinder centered at (0.2, 0.2) with radius 0.05, we can see Figure 1 for more details.

No slip boundary conditions are endowed on the top and bottom walls, and the inflow and outflow profiles are set as follows:

Table 1: Errors and convergence rates by using the Subgrid-Sparse-Div-Grad stabilization method with $T = 1, H = 2h, \Delta t = (1/20)h$, Re = 100.

$1/h$	$\|\|\|u - u_h\|\|\|_{\infty,0}$	Rate	$\|\|\|p - P_h\|\|\|_{2,0}$	Rate	$\|\|\|u - u_h\|\|\|_{2,1}$	Rate	$\|\|\|\nabla \cdot u_h\|\|\|_{2,0}$	Rate
4	0.0453001		0.209124		0.324832		0.101103	
8	0.00544822	3.05566	0.060671	1.78528	0.0718307	2.17702	0.0291351	1.79499
16	0.000544163	3.32368	0.00817061	2.89249	0.0148829	2.27094	0.00772961	1.91429
32	$4.6711e-005$	3.5422	0.000871184	3.22939	0.00329518	2.17523	0.0019698	1.97235
64	$3.64707e-006$	3.67895	0.000104475	3.05983	0.000769529	2.09831	0.000495154	1.9921
128	$3.78758e-007$	3.26739	$2.32851e-005$	2.16567	0.000181992	2.0801	0.000124009	1.99743

Table 2: Errors and convergence rates by using the Subgrid-Sparse-Div-Grad stabilization method with $T = 1, H = 2h, \Delta t = (1/20)h$, Re = 1000.

$1/h$	$\|\|\|u - u_h\|\|\|_{\infty,0}$	Rate	$\|\|\|p - P_h\|\|\|_{2,0}$	Rate	$\|\|\|u - u_h\|\|\|_{2,1}$	Rate	$\|\|\|\nabla \cdot u_h\|\|\|_{2,0}$	Rate
4	0.0561753		0.222197		0.382246		0.109382	
8	0.00788031	2.83361	0.0712768	1.64034	0.0973817	1.97278	0.0316068	1.79107
16	0.000979067	3.00877	0.0113473	2.65109	0.0227512	2.09771	0.00846383	1.90085
32	0.000113075	3.11413	0.00151224	2.90759	0.00482211	2.2382	0.00217781	1.95843
64	$1.25936e-005$	3.16651	0.000204634	2.88556	0.00104638	2.20426	0.000549488	1.98672
128	$1.29559e-006$	3.28102	$3.69974e-005$	2.46755	0.00024069	2.12016	0.000137294	2.00082

Table 3: Errors and convergence rates by using the Subgrid-Sparse-Div-Grad stabilization method with $T = 1, H = 2h, \Delta t = (1/20)h$, Re = 10000.

$1/h$	$\|\|\|u - u_h\|\|\|_{\infty,0}$	Rate	$\|\|\|p - P_h\|\|\|_{2,0}$	Rate	$\|\|\|u - u_h\|\|\|_{2,1}$	Rate	$\|\|\|\nabla \cdot u_h\|\|\|_{2,0}$	Rate
4	0.0573318		0.223624		0.388846		0.110302	
8	0.00820862	2.80412	0.0725471	1.62408	0.101548	1.93704	0.0318856	1.79048
16	0.00109348	2.90821	0.0118066	2.61932	0.0253046	2.00469	0.00855174	1.89862
32	0.000130748	3.06407	0.00163511	2.85214	0.00567973	2.15551	0.0022066	1.95439
64	$1.56252e-005$	3.06484	0.000233484	2.80799	0.00123601	2.20013	0.000559333	1.98004
128	$1.88945e-006$	3.04783	$4.27739e-005$	2.44852	0.00027947	2.14492	0.000140592	1.99219

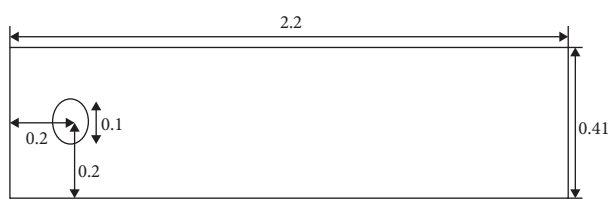

Figure 1: Computational domain for the two-dimensional flow past a cylinder.

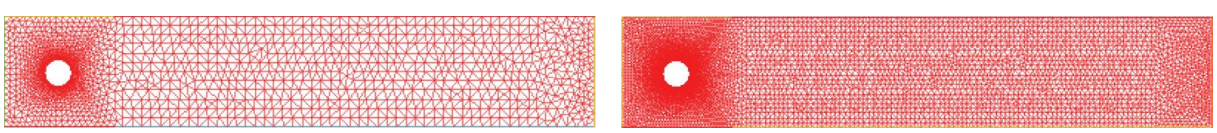

(a) (b)

Figure 2: The mesh used for computing flow around a cylinder. (a) The coarse mesh T_H. (b) The fine mesh T_h.

Table 4: The results of maximal drag/lift coefficients and pressure difference by using the Subgrid-Sparse-Div-Grad stabilization method.

Δt	$t_{c_{d,\max}}$	$c_{d,\max}$	$t_{c_{l,\max}}$	$c_{l,\max}$	$\Delta p(8\,s)$
0.01	3.95	2.94834	5.69	0.613275	−0.11232
0.005	3.94	2.94721	5.695	0.49686	−0.112598
0.001	3.937	2.94673	5.694	0.486905	−0.112503

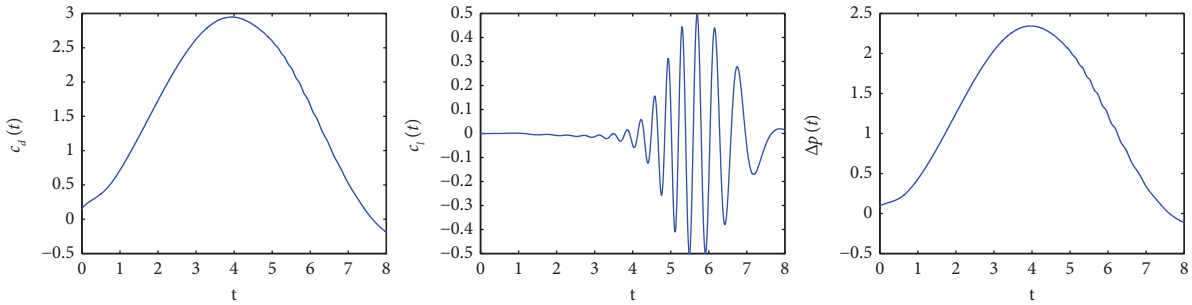

FIGURE 3: The development of $c_d(t), c_l(t)$ and $\Delta p(t)$ by the Subgrid-Sparse-Div-Grad stabilization method with $\Delta t = 0.005$, $\alpha(h) = h$, and $\gamma = 1$.

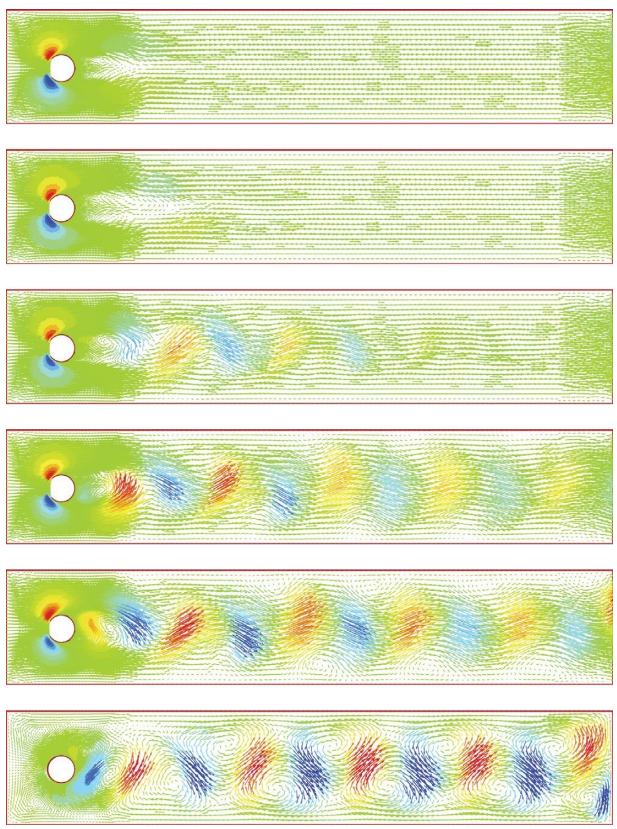

FIGURE 4: The velocity field at times $t = 2, 4, 5, 6, 7, 8$ for the NS equation solved by the Subgrid-Sparse-Div-Grad stabilization method with $\alpha(h) = h$ and $\gamma = 1$.

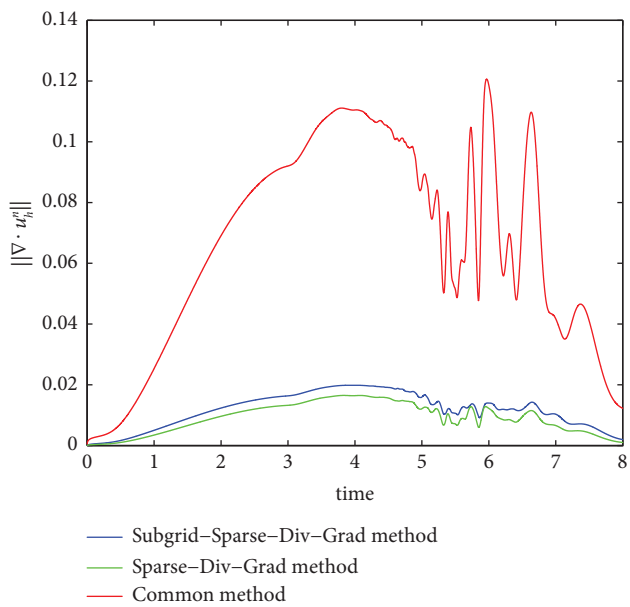

FIGURE 5: The development of $\|\nabla \cdot u_h^n\|$ by using different methods.

$$u_1(0, y, t) = u_1(2.2, y, t) = \frac{6}{0.41^2}\sin\left(\frac{\pi t}{8}\right) y(0.41 - y),$$
$$u_2(0, y, t) = u_2(2.2, y, t) = 0. \tag{66}$$

Taking the initial condition $u(x, y, 0) = 0$, the viscosity $\nu = 10^{-3}$, and the external force $f = 0$. Computations are implemented with final time $T = 8$. A fine mesh τ_h with 14508 triangulations and a coarse mesh τ_H with 3609 triangulations are given in Figure 2. And these meshes are used in this test.

The difference of pressure is defined by $\Delta p(t) = p(t; 0.15, 0.2) - p(t; 0.25, 0.2)$ and the drag and lift coefficients are defined as follows [34]:

$$c_d(t) = -20\int_\Omega \left[\nu \nabla u(t) : \nabla v_d + (u(t) \cdot \nabla) u(t) \cdot v_d - p(t)(\nabla \cdot v_d)\right] dx dy,$$
$$c_l(t) = -20\int_\Omega \left[\nu \nabla u(t) : \nabla v_l + (u(t) \cdot \nabla) u(t) \cdot v_l - p(t)(\nabla \cdot v_l)\right] dx dy, \tag{67}$$

where $v_d = (1, 0)^T$ on the nodes around the cylinder and vanishes everywhere else and $v_l = (0, 1)^T$ on the nodes around the cylinder and vanishes everywhere else.

The following reference intervals for the benchmark drag and lift coefficients are given in [34, 35] as:

$$c_{d,\max}^{\text{ref}} \in [2.93, 2.97], c_{l,\max}^{\text{ref}} \in [0.47, 0.49], \Delta p^{\text{ref}} \in [-0.115, -0.105]. \tag{68}$$

Table 4 shows $c_{d,\max}$ and $\Delta p(8\,s)$ are exactly in the interval of reference values, $c_{l,\max}$ is exactly in the benchmark interval when the time step size not too large. The evolutions of $c_d(t), c_d(t)$ and $\Delta p(t)$ with $\Delta t = 0.005$, $\alpha(h) = h$, $\gamma = 1$ by the Subgrid-Sparse-Div-Grad stabilization method are shown in Figure 3, which is in perfect agreement with with the results provided in [34]. The velocity field at times $t = 2, 4, 5, 6, 7, 8$ with $\alpha(h) = h$, $\gamma = 1$ are shown in Figure 4, we can see the vortex street forms successfully. Finally, a plot of $\|\nabla \cdot u_h^n\|$ vs. time for different methods is given in Figure 5, we can see that our method can keep mass conservation with time evolve.

6. Conclusions

In this article, we considered the synthesis of subgrid stabilization method with sparse div-grad stabilization method, derived the subgrid-sparse-grad-div stabilization method,

which is particularly efficient and maintains the best algorithmic features of each. The stability and convergence of this method were given. Numerical test verified the theoretical preconditions and demonstrated the effectiveness of the method. The application of the method to other coupled equations [39, 40] will be consider in the future.

Data Availability

All data that support the findings of this study can be obtained from the corresponding author upon request.

Conflicts of Interest

The authors declare that they have no conflicts of interest.

Acknowledgments

This work was supported by the Natural Science Foundation of China (NSFC) under grant no. 12161095, the Project of Yunnan Basic Research Program (Grant nos. 202001AU070068, 202201AT070032, and 202001AU070066), and the Yunnan Key Laboratory of Modern Analytical Mathematics and Applications (no. 202302AN360007).

References

[1] R. Temam, *Navie-Stokes Equations: Theory and Numerical Analysis*, North-Holland, Amsterdam, Netherlands, 1984.

[2] V. Girault and P. A. Raviart, *Finite Element Methods for Navier-Stokes Equations: Theory and Algorithms*, Springer-Verlag, Berlin, Germany, 1986.

[3] W. Layton, *Introduction to the Numerical Analysis of Incompressible Viscous Flows*, SIAM, Thailand, Asia, 2008.

[4] T. J. R. Hughes, L. Mazzei, and K. E. Jansen, "Large eddy simulation and the variational multiscale method," *Computer Vision and Image Understanding*, vol. 3, no. 1-2, pp. 47–59, 2000.

[5] V. John and S. Kaya, "Finite element error analysis of a variational multiscale method for the Navier-Stokes equations," *Advances in Computational Mathematics*, vol. 28, pp. 43–61, 2008.

[6] V. John and S. Kaya, "A finite element variational multiscale method for the Navier-Stokes equations," *SIAM Journal on Scientific Computing*, vol. 26, pp. 1485–1503, 2005.

[7] H. Zheng, Y. Hou, F. Shi, and L. Song, "A finite element variational multiscale method for incompressible flows based on two local Gauss integrations," *Journal of Computational Physics*, vol. 228, pp. 5961–5977, 2009.

[8] H. Zheng, Y. Hou, and F. Shi, "Adaptive variational multiscale methods for incompressible flow based on two local Gauss integrations," *Journal of Computational Physics*, vol. 229, pp. 7030–7041, 2010.

[9] J. Xu, "A novel two-grid method for semilinear elliptic equations," *SIAM Journal on Scientific Computing*, vol. 15, pp. 231–237, 1994.

[10] J. Xu, "Two-grid discretization techniques for linear and nonlinear PDEs," *SIAM Journal on Numerical Analysis*, vol. 33, pp. 1759–1777, 1996.

[11] S. Kaya and B. Riviere, "A two-grid stabilization method for solving the steady-state Navier-Stokes equations," *Numerical Methods for Partial Differential Equations*, vol. 22, pp. 728–743, 2006.

[12] J. L. Guermond, A. Marra, and L. Quartapelle, "Subgrid stabilized projection method for 2D unsteady flows at high Reynolds numbers," *Computer Methods in Applied Mechanics and Engineering*, vol. 195, pp. 5857–5876, 2006.

[13] W. Layton, "A connection between subgrid scale eddy viscosity and mixed methods," *Applied Mathematics and Computation*, vol. 133, pp. 147–157, 2002.

[14] S. Kaya, W. Layton, and B. Riviére, "Subgrid stabilized defect correction methods for the Navier-Stokes equations," *SIAM Journal on Numerical Analysis*, vol. 44, pp. 1639–1654, 2006.

[15] A. Çibik and S. Kaya, "A projection-based stabilized finite element method for steady-state natural convection problem," *Journal of Mathematical Analysis and Applications*, vol. 381, pp. 469–484, 2011.

[16] M. A. Belenli, S. Kaya, L. Rebholz, and N. E. Wilson, "A subgrid stabilization finite element method for incompressible magnetohydrodynamics," *International Journal of Computer Mathematics*, vol. 90, pp. 1506–1523, 2013.

[17] A. Çibik and S. Kaya, "Finite element analysis of a projection-based stabilization method for the darcy-brinkman equations in double-diffusive convection," *Applied Numerical Mathematics*, vol. 64, pp. 35–49, 2013.

[18] F. Yılmaz, "Semi-discrete a priori error analysis for the optimal control of the unsteady navier-stokes equations with variational multiscale stabilization," *Applied Mathematics and Computation*, vol. 276, pp. 127–142, 2016.

[19] M. Case, V. Ervin, A. Linke, and L. Rebholz, "A connection between scott-vogelius elements and grad-div stabilization taylor-hood FE approximations of the navier-stokes equations," *SIAM Journal on Numerical Analysis*, vol. 49, pp. 1461–1481, 2011.

[20] M. A. Olshanskii and A. Reusken, "Grad-Div stabilization for the stokes equations," *Mathematics of Computation*, vol. 73, pp. 1699–1718, 2004.

[21] E. W. Jenkins, V. John, A. Linke, and L. Rebholz, "On the parameter choice in grad-div stabilization for the Stokes equations," *Advances in Computational Mathematics*, vol. 40, pp. 491–516, 2014.

[22] A. Linke and L. Rebholz, "On a reduced sparsity stabilization of grad-div type for incompressible flow problems," *Computer Methods in Applied Mechanics and Engineering*, vol. 261, pp. 142–153, 2013.

[23] A. Bowers, S. Le Borne, and L. G. Rebholz, "Error analysis and iterative solvers for navier-stokes projection methods with standard and sparse grad-div stabilization," *Computer Methods in Applied Mechanics and Engineering*, vol. 275, pp. 1–19, 2014.

[24] A. Çıbık, "The effect of a sparse grad-div stabilization on control of stationary navier-sokes equations," *Journal of Mathematical Analysis and Applications*, vol. 437, pp. 613–628, 2016.

[25] J. A. Fiordilino, W. Layton, and Y. Rong, "An efficient and modular grad-div stabilization," *Computer Methods in Applied Mechanics and Engineering*, vol. 335, pp. 327–346, 2018.

[26] Y. Rong and J. A. Fiordilino, "Numerical analysis of a BDF2 modular grad-div stabilization method for the navier-stokes equations," *Journal of Scientific Computing*, vol. 82, p. 66, 2020.

[27] X. L. Lu and P. Z. Huang, "A modular grad-div stabilization for the 2D/3D nonstationary incompressible magnetohydrodynamic equations," *Journal of Scientific Computing*, vol. 82, p. 3, 2020.

[28] A. Labovschii, W. Layton, M. Manica, M. Neda, and L. Rebholz, "The stabilized extrapolated trapezoidal finite element method for the navier-stokes equations," *Computer Methods in Applied Mechanics and Engineering*, vol. 198, pp. 958–974, 2009.

[29] P. Hood and C. Taylor, "A numerical solution of the Navier-Stokes equations using the finite element technique," *Computers & Fluids*, vol. 1, pp. 73–100, 1973.
[30] M. Fortin, *Calcul numérique des ecoulements fluides de Bingham et des fluides Newtoniens incompressible par des méthodes d'eléments finis*, Springer, Berlin, Germany, 1972.
[31] S. Brenner and L. R. Scott, *The Mathematical Theory of Finite Element Methods*, Springer-Verlag, Berlin, Germany, 1994.
[32] J. G. Heywood and R. Rannacher, "Finite element approximation of the nonstationary navier-stokes problem. Part IV: error analysis for the second order time discretization," *SIAM Journal on Numerical Analysis*, vol. 27, pp. 353–384, 1990.
[33] F. Hecht, "New development in freefem++," *Journal of Numerical Mathematics*, vol. 20, no. 3-4, pp. 251–266, 2012.
[34] V. John, "Reference values for drag and lift of a two dimensional timedependent flow around a cylinder," *International Journal for Numerical Methods in Fluids*, vol. 44, pp. 777–788, 2004.
[35] M. Schäfer and S. Turek, "Benchmark computations of laminar flowaround a cylinder," in *Flow Simulations with High-Performance Computers II*, E. H. Hirschel, Ed., Springer, Berlin, Germany, 1996.
[36] G. Taylor, "On decay of vortices in a viscous fluid," *Philosophical Magazine*, vol. 46, pp. 671–674, 1923.
[37] G. Taylor and A. E. Green, "Mechanism of the production of small eddies from large ones," *Proceedings of the Royal Society of London Series A*, vol. 158, pp. 499–521, 1937.
[38] L. C. Berselli, "On the large eddy simulation of the taylor-green vortex," *Journal of Mathematical Fluid Mechanics*, vol. 7, pp. S164–S191, 2005.
[39] Y. B. Yang and Y. L. Jiang, "Numerical analysis and computation of a type of IMEX method for the time-dependent natural convection problem," *Computational Methods in Applied Mathematics*, vol. 16, pp. 321–344, 2016.
[40] Y. B. Yang, B. C. Huang, and Y. L. Jiang, "Error estimates of an operator-splitting finite element method for the time-dependent natural convection problem," *Numerical Methods for Partial Differential Equations*, vol. 39, pp. 2202–2226, 2023.